Single-Particle Tracking of Janus Colloids in Close Proximity

Stephen M. Anthony,[†] Minsu Kim,[‡] and Steve Granick*[,†,‡,§]

Departments of Chemistry, Physics, and Materials Science and Engineering, University of Illinois, Urbana, Illinois 61801

Received February 7, 2008. Revised Manuscript Received March 27, 2008

We describe algorithms and an experimental method based on differential interference contrast microscopy to discriminate optically anisotropic colloidal spheres under situations where diffraction owing to their close proximity causes overlapping images. The data analysis is applied to modulated optical nanoprobes (MOONs) that are coated with metal on one hemisphere. These methods enable single-particle tracking of rotation in addition to translation not only in concentrated suspensions but also in dilute suspensions when particles come into transient hydrodynamic contact. An illustrative example is given.

Introduction

One of the challenges of colloid science is to quantify not only the structural packing but also the rich dynamics of concentrated colloidal systems. It is a problem worthy of being solved because as colloidal particles are so ubiquitous in both nature and technology, to understand them is of widespread interest and potential utility. Yet, the major experimental advances made in recent years regarding the packing structure of colloidal glasses and crystals[1–4] are not yet fully matched by corresponding advances regarding orientational dynamical behavior at the single-particle level, partly owing to the difficulties of image analysis. For colloidal particles in dilute to moderately concentrated suspension, methods to locate individual particles have been established for a long time,[5] leading to exciting developments in comparing particle mobility to packing structure.

The now-traditional methods of colloidal tracking,[5] though capable of tracking everything from dilute solutions to glasses, are not designed to handle the consequences of optical anisotropy that arise on the introduction of modulated optical nanoparticles (MOONs) by Kopelman and co-workers.[6,7] Existing methods to deal with rotation are either restricted to effectively isolated particles[8] or to pairs of particles at carefully maintained separations larger than their diameter.[9] However, when dealing with MOON particles, the physical problem is to discriminate particles, coated with metal on one hemisphere in order to enable their rotation to be measured, under situations where their close proximity causes overlapping images and diffraction, which takes diverse forms depending upon the relative orientations of adjacent MOONs.

This article presents algorithms and an improved experimental approach to resolve this problem, which can happen not only in concentrated particle suspensions but also when low-concentration particles come into transient close contact in the course of Brownian motion, resulting in complex hydrodynamic forces such that solvent displacement and particle collisions mediate interactions between particles.[10,11] Previously, we introduced new techniques that allow the concurrent measurement of translation and rotation for optically anisotropic spheres of this kind,[8] but diffraction limits these methods to dilute situations where particles are widely separated in space. Here, we are interested primarily in spherical particles and present methods of image analysis simultaneously in "four dimensions" (two translational degrees and also two rotational degrees of freedom).

The image analysis methods introduced here represent a significant departure from traditional methods of colloidal tracking,[5] as they employ and extend overlapping object recognition algorithms.[12,13] Potentially, they can be useful when dealing with any colloidal system in which the particle images significantly overlap each other. On the experimental side, the use here of differential interference contrast (DIC) microscopy significantly extends the capability to monitor colloidal motion beyond what is possible using fluorescence labeling. This technique is normally used to resolve small differences of refractive index in the microscopy of unstained, translucent biological specimens. In this application to single-particle tracking of colloids, its advantage is to substantially increase the precision with which the center of MOON particles can be located, at the same time improving the resolution of one of the orientational degrees of freedom.

The potential significance is that these methods to simultaneously monitor translation and rotation of interacting particles open new avenues of exploration. While the translational hydrodynamic cross-correlation of particles has been studied,[10,14,15] comparable studies of rotational hydrodynamic cross-correlation have so far been limited to theory and computation of limited order[16,17] and have scarcely been explored experimentally at the single-particle level owing to the image analysis

[†] Department of Chemistry.
[‡] Department of Physics.
[§] Department of Materials Science and Engineering.

(1) Pusey, P. N.; Vanmegen, W. *Nature* **1986**, *320*, 340.
(2) Kegel, W. K.; van Blaaderen, A. *Science* **2000**, *287* (5451), 290.
(3) Leunissen, M. F.; Christova, C. G.; Hynninen, A. P.; Royall, C. P.; Campbell, A. I.; Imhof, A.; Dijkstra, M.; van Roij, R.; van Blaaderen, A. *Nature* **2005**, *437*, 235.
(4) Weeks, E. R.; Crocker, J. C.; Levitt, A. C.; Schofield, A.; Weitz, D. A. *Science* **2000**, *287*, 627.
(5) Crocker, J. C.; Grier, D. G. *J. Colloid Interface Sci.* **1996**, *179*, 298.
(6) Behrend, C. J.; Anker, J. N.; Kopelman, R. *Appl. Phys. Lett.* **2004**, *84*, 154.
(7) Behrend, C. J.; Anker, J. N.; McNaughton, B. H.; Brausel, M.; Philbert, M. A.; Kopelman, R. *J. Phys. Chem. B* **2004**, *108* (29), 10408.
(8) Anthony, S. M.; Hong, L.; Kim, M.; Granick, S. *Langmuir* **2006**, *22*, 9812.
(9) Martin, S.; Reichert, M.; Stark, H.; Gisler, T. *Phys. Rev. Lett.* **2006**, *97*, 248301.
(10) Meiners, J. C.; Quake, S. R. *Phys. Rev. Lett.* **1999**, *82*, 2211.
(11) Reichert, M.; Stark, H. *Phys. Rev. E* **2004**, *69*, 031407.
(12) Honkanen, M.; Saarenrinne, P.; Stoor, T.; Niinimaki, J. *Meas. Sci. Technol.* **2005**, *16*, 1760.
(13) Pla, F. *Comput. Vision Image Understanding* **1996**, *63*, 334.
(14) Cui, B. X.; Diamant, H.; Lin, B. H. *Phys. Rev. Lett.* **2002**, *89*, 188302.
(15) Cui, B. X.; Diamant, H.; Lin, B. H.; Rice, S. A. *Phys. Rev. Lett.* **2004**, *92*, 258301.
(16) Hermanns, H. G.; Felderhof, B. U. *J. Chem. Phys.* **2007**, *126*, 044902.
(17) Cichocki, B.; Ekiel-Jezewska, M. L.; Wajnryb, E. *J. Chem. Phys.* **1999**, *111*, 3265.

10.1021/la800424t CCC: $40.75
Published on Web 06/03/2008

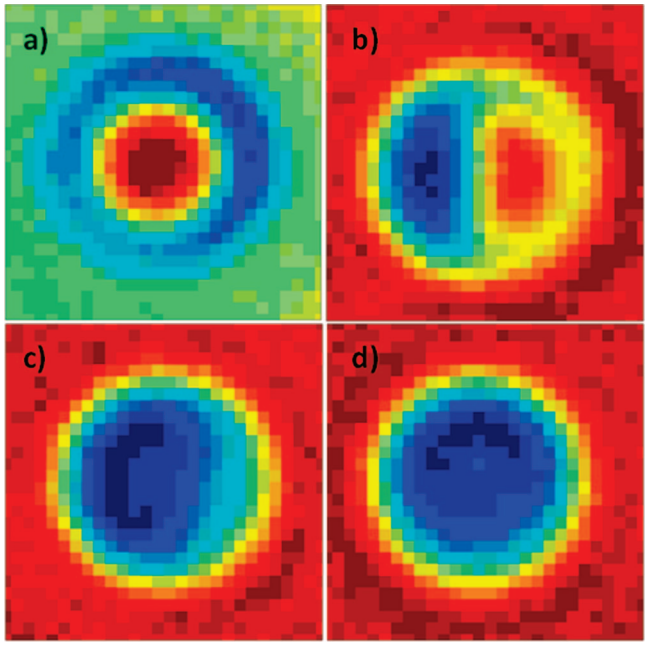

Figure 1. Sample DIC images showing an uncoated silica sphere (a) and MOON particles in "half moon" (b), "gibbous moon" (c), and "full moon" (d) orientations.

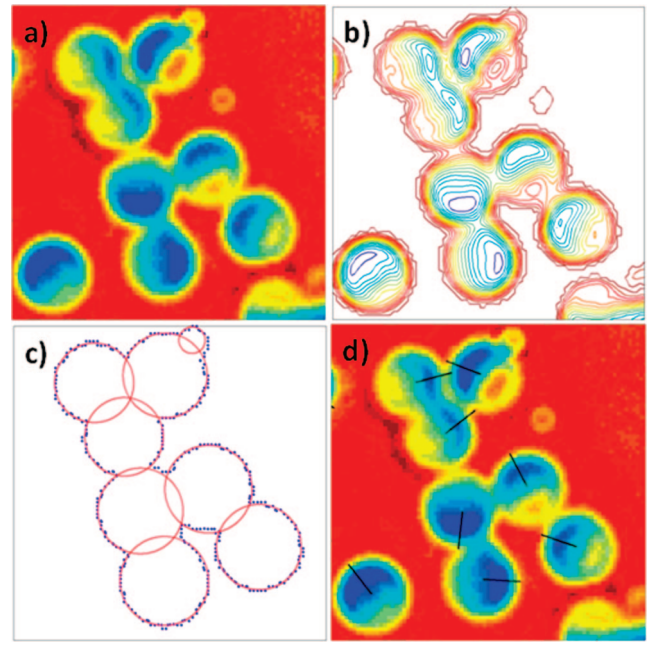

Figure 2. Demonstration of the general process to track optically anisotropic MOONs when images overlap. (a) Original image as recorded by the CCD camera. (b) Same image converted to contour plot form. For clarity, fewer contours are shown than are typically used in actual calculations. (c) Vertices of the exterior contour (blue dots) are fitted using an overlapping object recognition algorithm. This determines the circles of which the contour is composed (red circles). This procedure is robust, able to fit circles with half of their perimeter obscured. It recognizes particles of different sizes, including a piece of dust on the microscope objective (the small circle to the upper right). (d) Original image with overlaid black lines depicting the final fit. The lines run from the center of each particle outward, in this way indicating the angle (φ) in the plane of the image.

difficulties resolved here. With the developments presented here, translation and rotation can be measured simultaneously for almost the full range of concentrations, from dilute to just shy of the glass transition point for a 2D sample, where this method breaks down.

Experimental Section

Samples. Modulated optical nanoparticles (MOONs) were prepared by depositing reflective metal onto one hemisphere of monodisperse 1.57 μm silica microspheres (Duke Scientific 8150) following standard techniques.[18] Coating with 15 nm of aluminum oxide was selected because the density mismatch with silica is smaller than that of alternative reflective metals such as gold. This was followed by an additional coating of 15−20 nm of silicon oxide in order to render the MOON particles chemically homogeneous: bare silica on the uncoated hemisphere, matched with silicon oxide that covered the metal. The final variation in size of the colloids was less than 3% of their mean size. While, for these experiments, optically heterogeneous but chemically homogeneous Janus colloids were employed, the techniques are equally suitable to chemically heterogeneous Janus colloids. The MOONs were dispersed in an aqueous solution with ~1 mM salt, such that the Debye length was ~5 nm. The solution was deposited on a glass microscope slide, where under the influence of gravity the MOONs maintained an average separation of 200 nm from the surface.

Microscopy. Images were collected using a Zeiss Axiovert 200 instrument configured in differential interference contrast (DIC) mode using white light. A 100× objective was used, followed by 1.6× postmagnification. Dynamic data were recorded using a back-illuminated electron-multiplying charge-coupled device (CCD) camera (Andor iXON DV897-BV), with an exposure time of 16 ms per frame.

Results and Discussion

We begin with a few words about advantages and limitations of DIC imaging, particularly as this usage to image colloids is far afield from its traditional application. When observed under DIC, an untreated colloidal sphere of silica appears as shown in Figure 1 a. The center of the sphere is darker than the background and a bright halo surrounds the image, an indication of the substantial lensing caused by the sphere. Now contrast this to what happens when one hemisphere is coated with metal. The coated region is effectively opaque and casts a shadow (Figure 1b−d), varying with orientation. For all our measurements, our reference point on the MOON is the center of the coated hemisphere. The azimuthal angle φ is defined to be the angle in the xy image plane, with respect to the x-axis, with $0 \leq \varphi \leq 2\pi$. Correspondingly, the zenith angle θ should be the polar angle from the z-axis, with $0 \leq \theta \leq \pi$.[8] However, there is mirror-symmetry in the observed zenith angle; this is because, regardless of whether the hemispherical metal cap is oriented toward or away from the observer, the opaque region is effectively the same. The observed zenith angle θ then ranges from 0 to $\pi/2$ back to 0, as opposed to fluorescent MOONs, for which the full range of $0-\pi$ can be observed.[8] This is a disadvantage.

The main advantage is that, regardless of orientation, the entire perimeter of the MOON is resolvable from the background. This greatly simplifies locating particle position, particularly when particles are in close proximity to each other. Further, greater accuracy in determining the center also improves determination of the azimuthal angle φ. One further limitation is that multiple layers of MOONs would render the solution opaque, limiting this technique to either dilute solutions or 2D samples.

The algorithmic process of tracking MOONs in DIC mode consists of four major consecutive steps: (i) extracting the image information into a more concise form, (ii) approximately locating

(18) Anker, J. N.; Behrend, C. J.; Huang, H. M.; Kopelman, R. *J. Magn. Magn. Mater.* **2005**, *293*, 655.

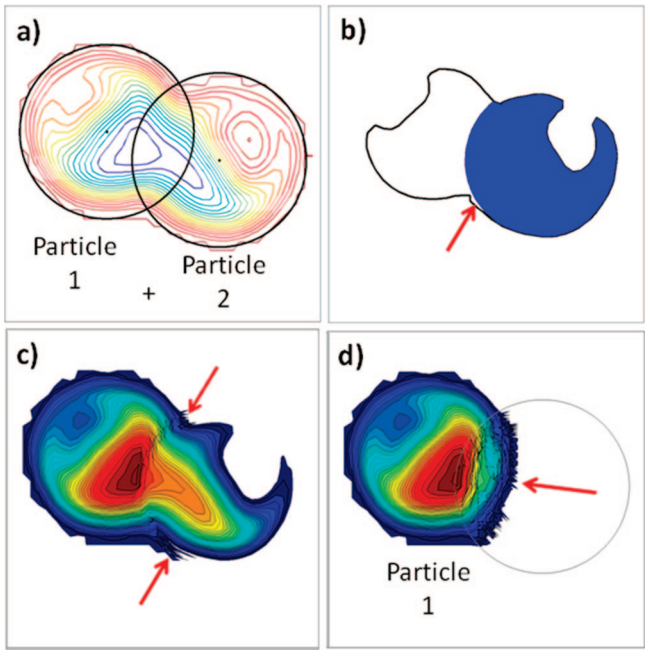

Figure 3. The technique to separate and resolve the elements of overlapping circular images is illustrated for a pair of particles. The Supporting Information (online) shows the iterative steps in movie format. In applying the method to more than the two particles illustrated here, the procedure is fundamentally the same. (a) The starting point is a contour plot of the overlapping images. Note that from using the overlapping object algorithm one knows approximately the position (shown here by dots) and diameter (shown here by black circles) of each particle. To begin, two copies of this initial contour plot are considered: one for particle 1 (left) one for particle 2 (right). (b) A contour from particle 2 (black line) has been selected, and a trial attempt was made to determine the portion of this contour that is genuinely attributable to particle 2 (blue area). This is subtracted from particle 1. Note that, because this approximation is inexact, slivers of particle 2 (red arrow) may not be subtracted. In subsequent iterations, this same procedure is applied to a contour from the new version of particle 1, iterating back and forth between the two particles. (c) Illustration of the imputed image of particle 1, partway through the iterative procedure. Notice that while the subtraction continues to improve relative to panel b, the slivers noted in panel b (red arrows) continue to accumulate. (d) After the iterations are completed, the image of particle 1 has been isolated. The slivers, whose presence in the earlier images was highlighted in the earlier panels of this figure, have been largely cropped off, using the criterion that they extend too far from the center of particle 1. Some image perturbation does remain from overlap with particle 2, whose position is indicated by the circle, but this is mostly roughness in the contour of the circles. This roughness is easy to notice visually but has minimal effect on subsequent calculations.

the position of each MOON, (iii) separating the overlapping MOON images, and (iv) extracting the more precise position and orientation from the now-isolated images.

Image Preprocessing. The first step in working with raw images is to deal with background and optical noise. To this end, a low pass filter is immediately applied (a standard boxcar filter, three pixels in each direction); this removes from the image some of the high-frequency noise. For this to be effective, the images should significantly exceed a few pixels in diameter. To put this in perspective, for the experiments described below, the typical apparent diameter of the MOONs was approximately 20 pixels including diffraction. Next, one subtracts the background. If the background intensity is relatively uniform, then since the intensity of the signal pixels varies dramatically compared to the background pixels, a histogram of the image brightness peaks at the mean value of the background. Properly binned, this can be identified as background and subtracted uniformly from all

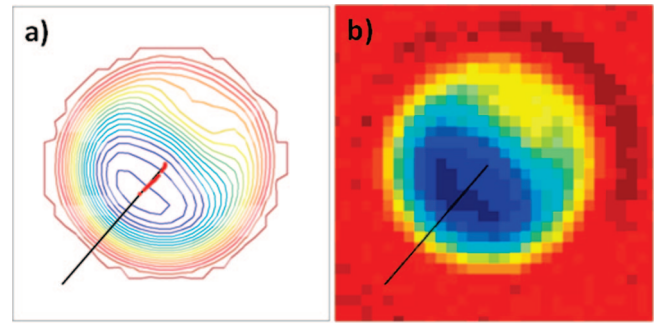

Figure 4. (a) Five most nearly circular contour rings are used to determine the center (terminus of the black line) of the particle. A linear fit to the centroids of each contour (red dots) yields the azimuth angle (black line) of the MOON. (b) Comparison of the raw image with the fit (black line).

pixels of the image. The image can then be transformed into a contour plot of lines whose intensity exceeds the background.

Overlapping Object Recognition. The next step is to approximately locate the position of each MOON. For any MOON or cluster of MOONs, the contour should consist of one or more overlapping circles (see Figure 2). To discriminate the circles, we employ standard algorithms for overlapping object recognition.[12,13] The basic overlapping object recognition algorithm employed here was described in depth by Honkanen et al.[12]

Several important modifications were made to account for our different application. The most critical is that we deal with overlapping circles rather than spheres; another capitalizes on the fact that the circles should possess nearly uniform size. At the same time, we could not just adopt the constant curvature method developed for circles by Pla,[13] as our contours are much smaller and noisier, so that curvature may not appear constant on any given length scale. Therefore, we employ the segmentation method of Honkanen et al.[12] Of the two clustering methods they mention, the one by Shen et al.[19] was more suitable for our purposes, as the noise level of our images often resulted in imperfect initial segmentation. This method assumes that if two circles overlap by a certain percentage, the overlapping segments should be considered part of the same circle. This criterion works well in our experiments, since the overlap between different MOONs arises primarily from diffraction and hence inherently is limited to a small fraction of the entire circle.

Finally, all segments are fit with a direct least-squares circle-fitting method. Further analysis is made only of those circles whose fitted diameter is close to the known diameter of the parent silica particles.

Separation of Overlapping MOONs. Up to this point of the image analysis, the images of MOONs in close proximity to one another still overlap owing to diffraction.

The distortion introduced from this overlap is significant. Even for simple silica spheres (not MOONs), it is known that traditional centroid-based tracking algorithms can overestimate the particle separation by up to tens or even hundreds of nanometers for this reason. A common method to correct it treats image overlap as a linear superposition and then exploits the symmetry of spheres by using a simple reflection algorithm to subtract contributions from adjacent particles.[20,21] This works well for pairs of particles but not for larger groupings of particles; the method is restricted

(19) Shen, L. P.; Song, X. Q.; Iguchi, M.; Yamamoto, F. *Pattern Recognit. Lett.* **2000**, *21*, 21.
(20) Verma, R.; Crocker, J. C.; Lubensky, T. C.; Yodh, A. G. *Macromolecules* **2000**, *33*, 177.
(21) Crocker, J. C.; Matteo, J. A.; Dinsmore, A. D.; Yodh, A. G. *Phys. Rev. Lett.* **1999**, *82*, 4352.

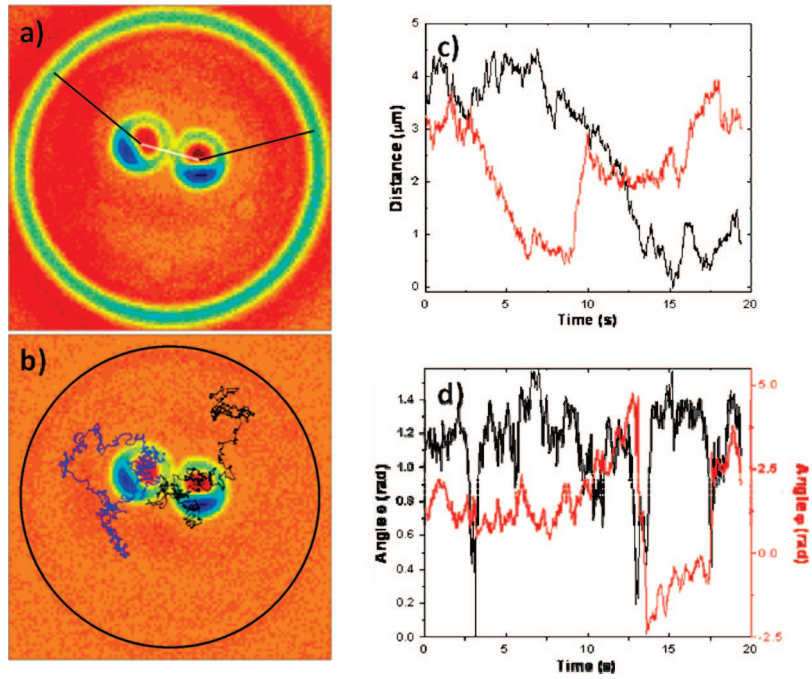

Figure 5. Illustrative example of applying the techniques introduced in this paper. Data of this kind are needed for subsequent analysis of the time-dependent hydrodynamic interactions between interacting colloidal particles. Here, particles 1.57 μm in diameter undergo quasi two-dimensional diffusion within a small circular corral, 10 μm in diameter, after they sediment in 1 mM PBS buffer of pH 7 onto the quartz slide to an average final wall−colloid spacing of ≈200 nm. (a) Illustrative DIC image of two particles. The black lines show the separation of the center of each MOON from the edge of the corral, and the white line shows the separation between the centers of the MOONs. (b) Same image after background subtraction to facilitate particle tracking. The black circle shows the position of the confining wall. The black and blue traces show the spatial trajectories of the particles during an illustrative time lapse of 20 s. (c) Wall−particle separation of each of the two particles, plotted against time. (d) Time-dependent orientation angles (φ, θ) for the same time series for the particle whose spatial position is plotted in black in panel c. Note that the abrupt changes in φ are reasonable, as small changes in the overall orientation of the particle result in large changes in φ when θ is close to 0. From data of this kind, it is straightforward to calculate the instantaneous translational and rotational velocity and, in turn, the instantaneous hydrodynamic forces between the colloidal particles and translation−rotation correlations, as will be reported elsewhere.

to relatively low particle concentration. In contrast, the method developed here (see Figure 3), while still assuming that image overlap is a linear superposition, uses an iterative subtraction process to separate and resolve the particles. This method can work with larger clusters of particles (see Figure 2) because it avoids the method of reflection. It is also well suited to handle the reduced symmetry of MOON particles.

The strategy proceeds as follows. Given a contour plot that consists of a linear superposition of the images of the two MOONs, one aims to subtract the image of one of them, thus revealing the image of the other. To accomplish this requires some bootstrapping because to implement it requires knowing the unperturbed image of one of the MOONs, exactly what we are trying to obtain. One can, however, make progress as follows. First, while one cannot yet work with the entire image, for those contours closest to the background, it is relatively easy to distinguish the contribution from each separate MOON, as the contour of each possesses a roughly circular region centered near the center of the MOON. Those contours whose intensity rises higher above the background consist of smaller circular regions, perhaps only a hemisphere or even less in the case of overlap between hemispheres on adjoining particles. Additionally, even without overlap from adjacent particles, these circles may be incomplete, unless the MOON is directly facing the observer. By fitting the circular portion, we determine the contribution from this MOON to the image of the other MOON (see Figure 3b).

In this iterative way, while one cannot directly subtract one MOON to leave the unperturbed image of the other, one subtracts one contour level at a time. In the process, each subsequent layer becomes less perturbed, such that, by subtraction of the final contour level, one deals with a nearly unperturbed contour (see Figure 3d). At each iteration, one uses image A to determine what to subtract from image B, and then image B is subtracted from image A, and so on iteratively. Subtractions are performed using the publicly available General Polygon Clipping library.[22]

Finally, one is left with relatively unperturbed images of each MOON. From experience, we have concluded that the portions subtracted correspond well to the opposing image (see the Supporting Information). It is important to note that the accuracy of this process is unaffected by the relative orientation of the neighboring MOONs. At the end, we are left with contour plots equivalent to those that would have been obtained from isolated MOONs at the same orientation and at the same position. Typical sequences of this iterative procedure are illustrated in the Supporting Information.

Refining the Position and Extracting the Orientation. Now, having in hand a reasonable estimate of the location of the center of each particle, it is easy to refine it, since the image is now that of an isolated MOON. Regardless of orientation, the contours closest to the background are complete circles. We obtain a more accurate center by fitting a circle to each of the five best such contours and then averaging all the centers obtained, yielding a final precision of <10 nm.

Next, the azimuth angle is determined. This proceeds from noticing that since the image must be symmetric across this angle, the centroid of each contour of the image must lie along the azimuth angle. Therefore, we compute the centroid of each

(22) Murta, A. *General Polygon Clipper Library*, version 2.31; http://www.cs.man.ac.uk/toby/alan/software/.

contour and then apply a linear fit to the centroids to determine the angle. The fit is trivially transformed from a line to a vector by determining which direction holds the highest intensity (see Figure 4).

Finally, the zenith angle is determined, based on the total intensity of the MOON after subtraction of the background. Determination of an exact formula equating intensity to angle is challenging here, as the silica particles act as sphere lenses, and it is necessary to account for both diffraction and interference. Here, instead, we make use of a convenient approximation, which corresponds to the portion of the image directly in line with the metal cap,

$$I = (A/2)(1 + \cos\theta) \quad (1)$$

Empirically, any deviation from this formula is less than our overall uncertainty in θ and hence can reasonably be ignored in most cases. This is unsurprising, since even when dealing with fluorescent MOONs emitting light from their entire volume,[8] which should exhibit much more substantial deviation, the deviation averages 4°.

Thus, for sufficiently long movies, it is possible to map intensities to angles, setting A equal to the intensity of the MOON at its highest, with two caveats. First, as can be seen from Figure 1, the DIC method applied here to silica spheres introduces some constant contribution to the intensity, particularly near the borders of the image. This contribution is quantified and subtracted from the image to generate a more accurate determination of the brightness. Second, one must realize that, when determining the zenith angle, images are equivalent whether a hemisphere is oriented toward or away from the observer. In spherical coordinates, computing the resulting uncertainty in orientation is a complex matter that we have not yet undertaken; the uncertainty frequently depends on the particle's orientation. Thus, while the accuracy of the zenith angle determined by the DIC method carries an unknown uncertainty, the uncertainty in determining the azimuth angle is improved relative to that based on fluorescence intensity.[8]

Illustrative Example. One aim of developing these methods is to analyze time-dependent hydrodynamic interactions between colloidal particles. A convenient experimental approach is to confine particles within a spherical corral into which they sediment and subsequently undergo quasi two-dimensional diffusion. Figure 5 shows illustrative spatial and rotational trajectories when two MOON particles (1.57 μm diameter) were confined within a spherical corral (10 μm diameter).

An image of an unprocessed image, at an instant of time when the two particles were close together near the center of the corral, is shown in Figure 5a. During the course of diffusion, the blue and black lines in Figure 5b show the trajectories of each particle as they wander throughout this closed area and sometimes approach the wall closely such that the particle image overlaps momentarily the image of the wall (the time lapse is 20 s). Figure 5c shows the time-dependent position of each particle, plotted against time. Notice that the positions were accurately quantified even when they approached close to the wall. In fact, the particles were well resolved not only when diffraction broadening caused images to overlap, but even when one particle rose momentarily in the vertical direction and partially eclipsed the other, leading to an interparticle separation of less than 1 diameter in the plane of the image. For these same data, Figure 5d shows the accompanying time-dependent azimuth angle (φ) and zenith angle (θ). Notice that the occasional abrupt changes are reasonable, as small changes in particle orientation appear as large changes in φ when θ is close to 0. From data of this kind, it is straightforward to calculate the instantaneous velocity and, in turn, the instantaneous hydrodynamic forces between the colloidal particles, as will be reported elsewhere. Studies of translation−rotation correlation are also enabled by data of this kind.

Acknowledgment. This work was supported by the U.S. Department of Energy, Division of Materials Science, under Award No. DE-FG02-07ER46471 through the Frederick Seitz Materials Research Laboratory at the University of Illinois at Urbana−Champaign. S.A. acknowledges the Donors of the Petroleum Research Fund, administered by the American Chemical Society, #45523-AC7, and also the NSF for financial support in the form of a Graduate Research Fellowship.

Supporting Information Available: Movie illustrating sequences of the iterative process to deduce the position and orientation of single MOON particles from images where multiple MOON particles are in such close proximity that their images overlap due to diffraction broadening. This material is available free of charge via the Internet at http://pubs.acs.org.

LA800424T